Nonlinear Control of a DC MicroGrid for the Integration of Photovoltaic Panels

Alessio Iovine, Sabah Benamane Siad, Gilney Damm, Elena de Santis, Maria Domenica Di Benedetto

Nonlinear Control of a DC MicroGrid for the Integration of Photovoltaic Panels

A. Iovine[a], S. B. Siad[b], G. Damm[b], E. De Santis[a], M. D. Di Benedetto[a]

***Abstract*—New connection constraints for the power network (Grid Codes) require more flexible and reliable systems, with robust solutions to cope with uncertainties and intermittence from renewable energy sources (renewables), such as photovoltaic arrays. The interconnection of such renewables with storage systems through a Direct Current (DC) MicroGrid can fulfill these requirements. A "Plug and Play" approach based on the "System of Systems" philosophy using distributed control methodologies is developed in the present work. This approach allows to interconnect a number of elements to a DC MicroGrid as power sources like photovoltaic arrays, storage systems in different time scales like batteries and supercapacitors, and loads like electric vehicles and the main AC grid. The proposed scheme can easily be scalable to a much larger number of elements.**

***Note to Practitioners*—Renewable energy can play a key role in producing local, clean and inexhaustible energy to supply the worlds increasing demand for electricity. Photovoltaic conversion of solar energy is a promising solution and is the best fit in several situations. However, its intermittent nature remains a real difficulty that can create instability. To answer to the new constraints of connection to the network (grid codes) for either solar plants than distributed generation, one possible solution is the use of Direct Current (DC) MicroGrids including storage systems, in order to integrate the electric power generated by these photovoltaic arrays. One of the main reasons is the fact that photovoltaic panels, batteries, supercapacitors and electric vehicles are DC. On the other hand, reliable stable control of DC MicroGrids is still an open problem. In particular it lacks rigorous analysis that can establish the operation regions and stability conditions for such MicroGrids. Current works that consider realistic grids usually apply from-the-shelf solutions that do not study the dynamics of such grids. While more rigorous studies just consider too much simplified grids that does not represent the conditions from real life applications. The present work presents nonlinear controllers capable to stabilize the DC MicroGrid, with rigorous analysis on the sufficient conditions and region of operation of the proposed control.**

***Keywords*—DC power systems, Power generation control, Photovoltaic power systems, Lyapunov methods**

I. INTRODUCTION

Renewable energy can play a key role in producing local, clean and inexhaustible energy to supply the world's increasing demand for electricity. Photovoltaic (PV) conversion of solar energy is a promising way to meet the growing demand for energy, and is the best fit in several situations [1]. However, its intermittent nature remains a real disability that can create voltage (or even frequency in the case of islanded MicroGrids) instability for large scale grids. In order to answer to the new constraints of connection to the network (Grid Codes) it is possible to consider storage devices [2], [3]; the whole system will be able to inject the electric power generated by photovoltaic panels to the grid in a controlled and efficient way. As a consequence, it is necessary to develop a strategy for managing energy in relation to the load and the storages constraints. Direct Current (DC) microgrids are attracting interest thanks to their ability to easily integrate modern loads, renewables sources and energy storages [4], [5], [6], [7], [8] since most of them (like electric vehicles, batteries and photovoltaic panels) are naturally DC: therefore, in this paper a DC microgrid composed by a source, a load, two storages working in different time scales, and their connecting devices is considered.

The utilized approach is based on a "Plug and Play" philosophy: the global control will be carried out at local level by each actuator, according to distributed control paradigm. The controller is developed in a distributed way for stabilizing each part of the whole system, while performing power management in real time to satisfy the production objectives while assuring the stability of the interconnection to the main grid.

Even if control techniques for converters are a well known research field [9], [10], [11], [12], the models generally used assume to have full controllability of the system [13], [14]; in reality, due to technical reasons, systems have an additional variable (a capacitor) on the source side [15]. Controlling this capacitor implies in leaving another variable (the grid side capacitor) uncontrolled; this remaining dynamics is usually neglected by the assumption that it is connected (and implicitly stabilized) by an always stable strong main grid. Removing this assumption to consider a realistic grid implies that this dynamics needs to be taken into account when studying grid stability. To the best of authors knowledge, no rigourous stability analysis has been developed for a realistic DC MicroGrid. In this paper convergence analysis is performed for all the dynamics composing each device with the target to extract a desired amount of power. In the same way, dynamics interaction is evaluated in order to obtain voltage stability in the DC MicroGrid in response to load and generation variations. Indeed as introduced in this paper, only a rigourous analysis of all the dynamics provide the grid stability conditions to be respected.

The adopted control strategy is shown to work both in case of time-varying uncontrolled load than in case of constant controlled load; both problems being relevant [16], [17]. The whole system provides protection against faults and suppresses interference, and has a positive impact on the behaviour of the

[a] Alessio Iovine, Elena De Santis and Marika Di Benedetto are with the Center of Excellence DEWS, Department of Information Engineering, Computer Science and Mathematics, University of L'Aquila, Italy. Email: alessio.iovine@graduate.univaq.it, {elena.desantis, mariadomenica.dibenedetto}@univaq.it. Corresponding author: Alessio Iovine. Permanent email: alessio.iovine@hotmail.com

[b] Gilney Damm and Sabah B. Siad are with IBISC - Universit d'Evry Val d'Essonne, Evry, France. Email: gilney.damm@ibisc.fr, siadsabah@yahoo.fr

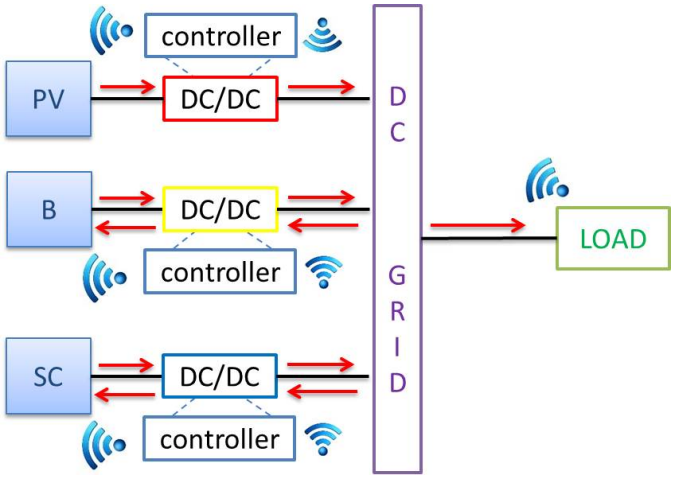

Figure 1. The considered framework

complete electrical system. The final management system can be configurable and adaptable as needed.

This paper is organized as follows. In Section III the model of the DC MicroGrid is introduced. Then in Section IV the adopted control laws for each subsystem are proven to satisfy stability requirements. Section V provides simulation results about the connected system behaviour, while in Section VI conclusions are provided.

II. Problem definition

The reference framework is depicted in Figure 1, where the isolated DC microgrid is represented. The targets would be to assure voltage DC grid stability while correctly feeding the load. To each element (PV array, battery, supercapacitor) a DC/DC converter is connected: their dynamical models are described in Section III. The whole control objective is then split in several tasks; the first one is to extract the maximum available power from the photovoltaic array. This maximum power production is obtained calculating the optimal value of the duty cycle in order to fix the PV array connected capacitor voltage to a given reference. Backstepping theory is used to stabilize the DC/DC boost converter that connects the solar array to the DC network.

The focus then moves to the storage systems and their connection to the DC network. In this paper, two kinds of storage are considered: a battery, which purpose is to provide/absorb the power when needed, and a supercapacitor, which purpose is to stabilize the DC grid voltage in case of disturbances. DC/DC bidirectional converters are necessary to enable the two modes of functioning (charge and discharge). The battery is assimilated as a reservoir which acts as a buffer between the flow requested by the network and the flow supplied by the production sources, and its voltage is controlled by the DC/DC current converter. Again, backstepping theory is used for designing the controller and assuring stability. With this structure, the DC grid is able to provide a continuous supply of good quality energy.

The three converters present in this system must, in a decentralized way, keep the stability of the DC network interconnecting all parts. The final management system can be configurable and adaptable as needed.

A. Assumptions

In this paper two main assumptions are made: the first one is the existence of a higher level controller which provide references to be accomplished by the local controllers [18]; the second one is about a proper sizing of each component of the microgrid in order to have feasible power balance.

1) ***Higher level controller****:* The power output coming from the sources needs to be properly coordinated and controlled. Here we assume that a higher level controller provides references for the local controllers: these references change every fixed time interval T and concern the amount of power needed for the next time interval and the desired voltage value for the DC grid. The time interval T is decided by the high level controller according to the computational time needed for calculations. These references are about the desired voltage to impose to the PV array and to the battery to obtain the needed amount of power, V_1^* and V_4^* respectively, and the desired voltage value for the DC grid, V_9^*. We need the references to be able to take into account a proper charge/discharge rate power for the supercapacitor; a state of charge about 50% at the beginning of the time interval is the best starting point for efficiency reasons.

2) ***Energy balance****:* Proper sizing of each component in a DC microgrid is an important feasibility requirement. In order to always satisfy the power demanded by the load, the sizing of the PV array, battery and supercapacitor fit some conditions related to the P_{PV} produced power by the photovoltaic array, the P_B and P_{SC} stored power into the battery and the supercapacitor respectively, and the P_L power absorbed by the load:

i) the sizing of the photovoltaic array is performed according to total energy needed into a whole day;

$$\int_0^D P_{PV}\, dt \geq \int_0^D P_L\, dt \tag{1}$$

where D is equal to daytime, 24 hours;

ii) the sizing of the battery and the supercapacitor are performed according to the energy balance in a T time step , needed for selecting a new reference;

$$\left\| \int_{kT}^{(k+1)T} (P_{PV} + P_B - P_L)\, dt \right\| \leq \frac{1}{2} \int_{kT}^{(k+1)T} P_{SC}\, dt \, \forall k \tag{2}$$

The last condition can be seen as the ability of the supercapacitor to fulfill the request to provide enough amount of power in the considered time interval; for sizing the supercapacitor we consider the worst scenario due to current load variations, i.e. the case where the supercapacitor needs to provide/absorb the maximum available current for all the time step.

The complete sizing of these components is considered out of the scope at this point, and will be studied in future works.

III. DC MicroGrid modeling

In this Section the considered framework depicted in Figure 1 is described. The PV array, battery and supercapacitor are

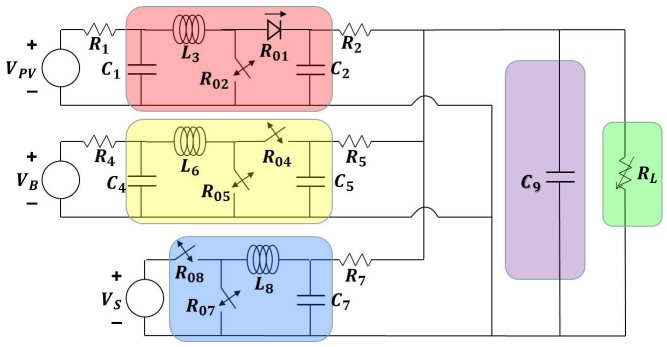

Figure 2. The interconnected system.

each one connected to the DC grid by a DC/DC converter. Here the circuital representation and the mathematical model are given, based on power electronics averaging technique [19], [20].

$$\dot{x}(t) = f(x(t)) + g(x(t), u(t), d(t)) + d(t) \tag{3}$$

$$x = \begin{bmatrix} x_1 & x_2 & x_3 & x_4 & x_5 & x_6 & x_7 & x_8 & x_9 \end{bmatrix}^T \tag{4}$$

$$u = \begin{bmatrix} u_1 & u_2 & u_3 \end{bmatrix}^T \tag{5}$$

$$d = \begin{bmatrix} V_{PV} & V_B & V_S & \dfrac{1}{R_L} \end{bmatrix}^T \tag{6}$$

$$\begin{cases} \dot{x}_1 = -\frac{1}{R_1 C_1} x_1 - \frac{1}{C_1} x_3 + \frac{1}{R_1 C_1} V_{PV} \\ \dot{x}_2 = -\frac{1}{R_2 C_2} x_2 + \frac{1}{C_2} x_3 - \frac{1}{C_2} u_1 x_3 + \frac{1}{R_2 C_2} x_9 \\ \dot{x}_3 = \frac{1}{L_3} \left[x_1 - x_2 - R_{01} x_3 \right] \\ \qquad + \frac{1}{L_3} (x_2 + (R_{01} - R_{02}) x_3) u_1 \\ \dot{x}_4 = -\frac{1}{R_4 C_4} x_4 - \frac{1}{C_4} x_6 + \frac{1}{R_4 C_4} V_B \\ \dot{x}_5 = -\frac{1}{R_5 C_5} x_5 + \frac{1}{C_5} x_6 - \frac{1}{C_5} u_2 x_6 + \frac{1}{R_5 C_5} x_9 \\ \dot{x}_6 = \frac{1}{L_6} x_4 - \frac{1}{L_6} x_5 - \frac{R_{04}}{L_6} x_6 + \frac{1}{L_6} x_5 u_2 \\ \dot{x}_7 = -\frac{1}{R_7 C_7} x_7 - \frac{1}{C_7} x_8 + \frac{1}{R_7 C_7} x_9 \\ \dot{x}_8 = \frac{1}{L_8} V_S u_3 - \frac{R_{08}}{L_8} x_8 - \frac{1}{L_8} x_7 \\ \dot{x}_9 = \frac{1}{C_9} \left[\frac{x_2 - x_9}{R_2} + \frac{x_5 - x_9}{R_5} + \frac{x_7 - x_9}{R_7} - x_9 \frac{1}{R_L} \right] \end{cases} \tag{7}$$

Here x_9 represents the voltage $V_{C_9} : \mathcal{R} \to \mathcal{R}^+$ of the capacitor C_9, which is the DC microgrid (depicted in violet in Figure 2. Such voltage is influenced by the connections with load and sources: $R_L \in \mathcal{R}^+$ is a constant value representing the load resistance, while the positive values of R_2, R_5, R_7 are the resistances among the dynamics x_9 and the interconnected dynamics x_2, x_5 and x_7. These dynamics are the voltages $V_{C_2} : \mathcal{R} \to \mathcal{R}^+$, $V_{C_5} : \mathcal{R} \to \mathcal{R}^+$ and $V_{C_7} : \mathcal{R} \to \mathcal{R}^+$ of the capacitors C_2, C_5 and C_7, which are components of the three DC/DC converters connected, respectively, to the PV array (red area), the battery (yellow area) and the supercapacitor (blue area) depicted in Figure 2. Their description is introduced in the following.

A. PV branch

The DC/DC converter needed to connect the PV array to the DC grid is a boost converter: it is illustrated in the red area in Figure 2. The equivalent circuit representation for the boost converter can be expressed using a state space average model. Three state variables are needed for the system model: the capacitor voltages $V_{C_1} : \mathcal{R} \to \mathcal{R}^+$ and $V_{C_2} : \mathcal{R} \to \mathcal{R}^+$ (x_1 and x_2 respectively) and the inductor current $I_{L_3} : \mathcal{R} \to \mathcal{R}$ (x_3). C_1, C_2, R_1, R_2, L_3, R_{01}, R_{02} are known positive values of the capacitors, resistances and the inductor while the disturbance $V_{PV} \in \mathcal{R}^+$, is the photovoltaic panel voltage. The measured signals are the states x_1, x_2, x_3 and the PV array voltage V_{PV}. u_1 is the control input, which is defined as the duty cycle of the circuit; its target is to properly integrate the power coming form the PV array and at the same time to obtain the maximum amount of power from the solar energy. This is known as the Maximum Power Point Tracking (MPPT) and consists to regulate the voltage V_{C_1} to its reference $V_1^* = x_1^*$ given by a higher level controller, and considered constant during each time interval T.

B. Battery branch

The DC/DC converter connecting the battery to the DC grid is a bidirectional converter: it is illustrated in the yellow area in Figure 2. As for the boost converter, we select three state variables: the capacitor voltages $V_{C_4} : \mathcal{R} \to \mathcal{R}^+$ and $V_{C_5} : \mathcal{R} \to \mathcal{R}^+$ (x_4 and x_5 respectively) and the inductor current $I_{L_6} : \mathcal{R} \to \mathcal{R}$ (x_6). C_4, C_5, R_4, R_5, L_6, R_{06} are known positive values of the circuit while the disturbance $V_B \in \mathcal{R}^+$ is the battery voltage. The measured signals are the states x_4, x_5, x_6 and the battery voltage V_B. The duty cycle u_2 is the control input; its target is to assign the reference $V_4^* = x_4^*$ value to x_4, forcing the battery to provide/absorb a desired amount of power, in a smooth way that maximizes its lifetime. This reference value is given by a higher controller not considered in the present paper, and is considered as constant during the time period T.

C. Supercapacitor branch

The DC/DC converter connecting the supercapacitor to the DC grid is a buck one[1]. Only two state variables are needed, x_7 for the capacitor voltage $V_{C_7} : \mathcal{R} \to \mathcal{R}^+$ and x_8 for the inductor current $I_{L_8} : \mathcal{R} \to \mathcal{R}$. The positive values of C_7, R_7, R_8, L_8, R_{08}, and the disturbance $V_S : \mathcal{R} \to \mathcal{R}^+$ (supercapacitor voltage) are known at each t. The model describing the evolution of the supercapacitor voltage is taken as in [21]. The duty cycle u_3 is the control input for this system. Its target is to control the capacitor voltage directly

[1]The converter used for the supercapacitor has different constraints from the one used for the battery, and for this reason is of a different topology.

connected to the grid, which is x_7. The measured signals are the states x_7, x_8, and the supercapacitor voltage $V_S(t) > 0$.

IV. Grid control

In this section control laws are derived to fit the desired targets: for each DC/DC converter a proper control action is developed and the interconnection among all of them is then used to ensure grid stability. Let us consider the state x, whose dynamics are described in (7). Let us consider the set of all possible values of x_1^* that generate a non negative current coming from the PV array as $x_1^* \in [\gamma_1 V_{PV}, V_{PV}]$, where $\gamma_1 = \frac{R_{01}}{R_1}\frac{1}{1+\frac{R_{01}}{R_1}}$. Given a positive value of R_L and x_9^*, let us moreover consider the set of all positive values of x_4^* such that the balance of the currents is expressed by

$$\frac{1}{R_L}x_9^* = \frac{1}{R_2}(x_2^* - x_9^*) + \frac{1}{R_5}(x_5^* - x_9^*) \tag{8}$$

where the values of x_2^* and x_5^* are defined as

$$x_2^* = \frac{x_9^* - a_2}{2} + \frac{1}{2}\sqrt{(x_9^* - a_2)^2 + 4R_2C_2(\Delta_2 + a_2 x_9^*)} \tag{9}$$

$$\Delta_2 = \frac{1}{R_1C_2}(V_{PV} - x_1^*)\left[x_1^* - \frac{R_{02}}{R_1}(V_{PV} - x_1^*)\right] \tag{10}$$

$$a_2 = \frac{R_{01} - R_{02}}{R_1}(V_{PV} - x_1^*) \tag{11}$$

$$x_5^* = \frac{x_9^*}{2} + \frac{1}{2}\sqrt{x_9^{*2} + 4R_5C_5\Delta_5} \tag{12}$$

$$\Delta_5 = \frac{1}{R_4C_5}(V_B - x_4^*)\left[-x_4^* + R_{04}\frac{1}{R_4}(V_B - x_4^*)\right] \tag{13}$$

and represent the solution of the dynamics x_2 and x_5 in equation (7) setting $\dot{x} = 0$

Theorem 1: For any given $x_1^* \in [\gamma_1 V_{PV}, V_{PV}]$, for any given $x_9^* > 0$, for any given $x_4^* > 0$ such that condition (8) is satisfied, under the assumption that for each t the conditions

$$x_2 + (R_{01} - R_{02})x_3 \neq 0, \quad x_5 \neq 0, \quad x_9 \neq 0 \tag{14}$$

hold, there exist control laws u_1, u_2 and u_3 such that the closed loop system has an equilibrium point in x^e:

$$x^e = \begin{bmatrix} x_1^e \\ x_2^e \\ x_3^e \\ x_4^e \\ x_5^e \\ x_6^e \\ x_7^e \\ x_8^e \\ x_9^e \end{bmatrix} = \begin{bmatrix} x_1^* \\ x_2^* \\ \frac{1}{R_1}(V_{PV} - x_1^*) \\ x_4^* \\ x_5^* \\ \frac{1}{R_4}(V_B - x_4^*) \\ x_9^* \\ 0 \\ x_9^* \end{bmatrix}. \tag{15}$$

Moreover, any evolution starting from any (admissible) initial condition $x(0)$ asymptotically converges to it.

Proof 1: The proof is based on the use of a Lyapunov function V which is a composition of different Lyapunov functions, as illustrated in [22], [23]. We use Proportional Integral (PI) control inputs u_1 and u_2 for properly controlling dynamics x_1, x_3, x_4 and x_6 in order to obtain a desired amount of power coming from the PV array and the battery. Then the control input u_3 focuses on the grid voltage regulating the interconnection among the systems. The control laws are developed by using a backstepping technique. The proposed Lyapunov function is

$$V = V_{1,3} + V_{4,6} + V_7 + V_8 + V_{2,5,9} \tag{16}$$

where all the terms are defined as follows.

Let us first focus on the control u_1, which is dedicated to dynamics x_1 and x_3: it is defined as

$$u_1 = \frac{1}{x_2 + (R_{01} - R_{02})x_3}\left[-x_1 + x_2 + R_{01}x_3 - L_3 v_1\right] \tag{17}$$

with

$$v_1 = K_3(x_3 - z_3) + \overline{K}_3\alpha_3 - C_1\overline{K}_1K_1^\alpha(x_1 - x_1^*) + \\ + \left(C_1K_1 - \frac{1}{R_1}\right)(K_1(x_1 - x_1^*) + \overline{K}_1\alpha_1) \tag{18}$$

$$z_3 = \frac{1}{R_1}(V_{PV} - x_1) + C_1K_1(x_1 - x_1^*) + C_1\overline{K}_1\alpha_1 \tag{19}$$

where the positive gains K_3, $\overline{K}_3$, K_3^α, $\overline{K}_1$, K_1^α, K_1, have to be properly chosen and α_1, α_3 are integral terms assuring zero error in steady state:

$$\dot{\alpha}_1 = K_1^\alpha(x_1 - x_1^*) \qquad \dot{\alpha}_3 = K_3^\alpha(x_3 - z_3) \tag{20}$$

An augmented system can be considered for the dynamics x_1 and x_3, where the state, the disturbance vector and the relating matrices are

$$\bar{x}_{1,3} = [\ x_1\ \ \alpha_1\ \ x_3\ \ \alpha_3\ ]^T \tag{21}$$

$$\bar{d}_{1,3} = [\ V_{PV}\ \ x_1^*\ ]^T \tag{22}$$

$$\dot{\bar{x}}_{1,3} = A_{1,3}\bar{x}_{1,3} + D_{1,3}\bar{d}_{1,3} \tag{23}$$

$$A_{1,3} = \begin{bmatrix} -\frac{1}{R_1C_1} & 0 & -\frac{1}{C_1} & 0 \\ K_1^\alpha & 0 & 0 & 0 \\ a_{31} & a_{32} & -K_3 & -\overline{K}_3 \\ K_3^\alpha\left(\frac{1}{R_1} - C_1K_1\right) & -K_3^\alpha C_1\overline{K}_1 & K_3^\alpha & 0 \end{bmatrix} \tag{24}$$

$$a_{31} = (K_3 - K_1)\left(C_1K_1 - \frac{1}{R_1}\right) + C_1\overline{K}_1K_1^\alpha \tag{25}$$

$$a_{32} = \overline{K}_1\left(K_3C_1 - K_1C_1 + \frac{1}{R_1}\right) \tag{26}$$

$$D_{1,3} = \begin{bmatrix} \frac{1}{R_1C_1} & 0 \\ 0 & -K_1^\alpha \\ \frac{K_3}{R_1} & d_{32} \\ -\frac{K_3^\alpha}{R_1} & C_1K_1K_3^\alpha \end{bmatrix} \tag{27}$$

$$d_{32} = -C_1\overline{K}_1K_1^\alpha + K_1\left(C_1K_1 - K_3C_1 - \frac{1}{R_1}\right) \tag{28}$$

System (23) has the following equilibrium points:

$$\bar{x}_{1,3}^e = \begin{bmatrix} x_1^*\ \ 0\ \ \frac{V_{PV} - x_1^*}{R_1}\ \ 0 \end{bmatrix}^T \tag{29}$$

The characteristic polynomial is considered; to obtain stability all the terms need to be strictly positive, i.e. $p_3 > 0$, $p_2 > 0$, $p_1 > 0$, $p_0 > 0$.

$$p(\lambda) = \lambda^4 + p_3\lambda^3 + p_2\lambda^2 + p_1\lambda + p_0 \tag{30}$$

Table I
ROUTH TABLE

1	p_2	p_0
p_3	p_1	0
$p_2 - \frac{p_1}{p_3}$	$p_o p_1 \frac{1}{p_3}$	
$p_2 - p_0 p_1 \frac{1}{p_2 - \frac{p_1}{p_3}}$		

$$p_3 = K_3 + \frac{1}{R_1 C_1} > 0 \tag{31}$$

$$p_2 = \overline{K}_3 K_3^\alpha + \frac{1}{R_1 C_1} K_3 + \overline{K}_1 K_1^\alpha + \\ + \left[(K_3 - K_1) \left(K_1 - \frac{1}{R_1 C_1} \right) \right] > 0 \tag{32}$$

$$p_1 = \frac{1}{R_1 C_1} \left(\overline{K}_3 K_3^\alpha + \overline{K}_1 K_1^\alpha \right) + \\ + \overline{K}_1 K_1^\alpha (K_3 - K_1) + K_3^\alpha \left(K_1 - \frac{1}{R_1 C_1} \right) > 0 \tag{33}$$

$$p_0 = \overline{K}_1 \overline{K}_3 K_3^\alpha K_1^\alpha > 0 \tag{34}$$

Due to the hypothesis of positive gains, conditions (31) and (34) are always satisfied; furthermore, $K_3 > K_1$ and $K_1 > \frac{1}{R_1 C_1}$ are sufficient conditions for the (33) and (32) to be respected. Other conditions are given by the Routh criterium in Table I.

$$p_2 > \frac{p_1}{p_3} \tag{35}$$

$$p_2 - \frac{p_0 p_1}{p_2 - \frac{p_1}{p_3}} > 0 \tag{36}$$

It can be shown that these conditions can be fulfilled with a proper choice of the parameter K_3. We do not include here the corresponding calculations for lack of space. As a result, an asymptotically stable linear system is obtained; then there will exist a Lyapunov function $V_{1,3}$ in the form of

$$V_{1,3} = \frac{1}{2} (\bar{x}_{1,3} - \bar{x}_{1,3}^e)^T P_{1,3} (\bar{x}_{1,3} - \bar{x}_{1,3}^e) > 0 \tag{37}$$

with

$$\dot{V}_{1,3} < 0 \tag{38}$$

where the symmetric positive definite matrix $P_{1,3}$ is obtained by the Riccati equation $A_{1,3}^T P_{1,3} + P_{1,3} A_{1,3} = -Q_{1,3}$ such that (38) is verified.

The control input u_2, which is dedicated to control the dynamics x_4 and x_6 and to ensure a desired charge/discharge behaviour of the battery imposing the reference x_4^*, is of the form of

$$u_2 = \frac{1}{x_5} \left(-x_4 + x_5 + R_{04} x_6 + L_6 v_2 \right) \tag{39}$$

with

$$v_2 = - K_6 (x_6 - z_6) - \overline{K}_6 \alpha_6 + \overline{K}_4 K_4^\alpha (x_4 - x_4^*) + \\ - \left(C_4 K_4 - \frac{1}{R_4} \right) \left(K_4 (x_4 - x_4^*) + \overline{K}_4 \alpha_4 \right) \tag{40}$$

where the positive gains K_6, $\overline{K}_6$, K_6^α, $\overline{K}_4$, K_4^α, K_4, are properly chosen and

$$z_6 = \left(\frac{1}{R_4} (V_B - x_4) + C_4 K_4 (x_4 - x_4^*) + C_4 \overline{K}_4 \alpha_4 \right) \tag{41}$$

$$\dot{\alpha}_4 = K_4^\alpha (x_4 - x_4^*) \qquad \dot{\alpha}_6 = K_6^\alpha (x_6 - z_6) \tag{42}$$

with α_4 and α_6 being integral terms assuring zero error in steady state.

As for the previous case, an augmented system can be considered:

$$\dot{\bar{x}}_{4,6} = A_{4,6} \bar{x}_{4,6} + D_{4,6} \bar{d}_{4,6} \tag{43}$$

$$\bar{x}_{4,6} = [\ x_4\ \ \alpha_4\ \ x_6\ \ \alpha_6\ ]^T \tag{44}$$

$$\bar{d}_{4,6} = [\ V_B\ \ x_4^*\ ]^T \tag{45}$$

The system in (43) has matrices $A_{4,6}$ and $D_{4,6}$ similar to $A_{1,3}$ and $D_{1,3}$ in (23), with respect to the considered gains. The same considerations drive to the same asymptotic stability result; then there will exist a Lyapunov function $V_{4,6}$ in the form of

$$V_{4,6} = \frac{1}{2} (\bar{x}_{4,6} - \bar{x}_{4,6}^e)^T P_{4,6} (\bar{x}_{4,6} - \bar{x}_{4,6}^e) > 0 \tag{46}$$

with

$$\dot{V}_{4,6} < 0 \tag{47}$$

where the symmetric positive definite matrix $P_{4,6}$ is obtained by the Riccati equation $A_{4,6}^T P_{4,6} + P_{4,6} A_{4,6} = -Q_{4,6}$ such that (47) is verified.

Let us now focus on the control input u_3, which is determined to ensure voltage grid stability. It does not act directly. It does not act directly on the DC grid, but through the dynamics x_8 and x_7. Utilizing backstepping and Lyapunov methods, we can select the desired value for the dynamics to control the grid. The Lyapunov functions provided at each step will be used for the entire system, thereby leading to the study of composite Lyapunov functions.

The function $V_{2,5,9}$ refers to dynamics x_2, x_5 and x_9; introducing the errors e_2 and e_5 between the dynamics and their equilibrium points as

$$e_2 = x_2 - x_2^*, \qquad e_5 = x_5 - x_5^*$$

we can rewrite the equations as

$$\begin{cases} \dot{e}_2 = \frac{1}{R_2 C_2} (x_9 - e_2 - x_2^*) + \frac{1}{C_2} x_3 (1 - u_1) \\ \dot{e}_5 = \frac{1}{R_5 C_5} (x_9 - e_5 - x_5^*) + \frac{1}{C_5} x_6 (1 - u_2) \\ \dot{x}_9 = \frac{1}{C_9} \left(\frac{1}{R_2} (e_2 + x_2^* - x_9) + \frac{1}{R_5} (e_5 + x_5^* - x_9) \right) + \\ + \frac{1}{C_9} \left(\frac{1}{R_7} (x_7 - x_9) - \frac{1}{R_L} x_9 \right) \end{cases} \tag{48}$$

To find a proper controller, the $V_{2,5,9}$ can be defined as

$$V_{2,5,9} = \frac{C_2}{2} e_2^2 + \frac{C_5}{2} e_5^2 + \frac{C_9}{2} x_9^2 \tag{49}$$

Then,

$$\dot{V}_{2,5,9} = -\frac{1}{R_2}e_2^2 + e_2\left(\frac{1}{R_2}(x_9 - x_2^*) + x_3(1-u_1)\right) + \tag{50}$$
$$- \frac{1}{R_5}e_5^2 + e_5\left(\frac{1}{R_5}(x_9 - x_5^*) + x_6(1-u_2)\right)$$
$$+ x_9\left(\frac{1}{R_2}(e_2 + x_2^* - x_9) + \frac{1}{R_5}(e_5 + x_5^* - x_9)\right) +$$
$$+ x_9\left(\frac{1}{R_7}(x_7 - x_9) - \frac{1}{R_L}x_9\right)$$

In equation (50) the dynamics x_7 can be seen as control input; it can be properly chosen to obtain a desired form for the $\dot{V}_{2,5,9}$. By choosing the value z_7 for x_7 as

$$z_7 = -R_7\frac{1}{x_9}\left[e_2\left(\frac{1}{R_2}(x_9 - x_2^*) + x_3(1-u_1)\right)\right] + \tag{51}$$
$$- R_7\frac{1}{x_9}\left[e_5\left(\frac{1}{R_5}(x_9 - x_5^*) + x_6(1-u_2)\right)\right] +$$
$$+ R_7\left[\frac{x_9}{R_L} - \frac{1}{R_2}(e_2 + x_2^* - x_9) - \frac{1}{R_5}(e_5 + x_5^* - x_9)\right] +$$
$$+ \frac{1}{x_9}\left(-{x_9^*}^2 + 2x_9x_9^*\right)$$

the $\dot{V}_{2,5,9}$ results to be semidefinite negative. To prove asymptotic stability the set Ω is considered: it is the largest invariant set of the set E of all points where the Lyapunov function is not decreasing. Ω contains an unique point; then applying LaSalle's theorem asymptotic stability of the equilibrium point can be established.

$$\dot{V}_{2,5,9} = -\frac{1}{R_2}e_2^2 - \frac{1}{R_5}e_5^2 - \frac{1}{R_7}(x_9 - x_9^*)^2 \leq 0 \tag{52}$$

$$\Omega = \{(e_2, e_5, x_9) \,:\, x_2 = x_2^*,\, x_5 = x_5^*,\, x_9 = x_9^*\} = \tag{53}$$
$$= \{(0, 0, x_9^*)\}$$

In order to calculate $z_8(t)$ such that x_8 backsteps the value of x_7 to the desired value z_7, we use the Lyapunov function

$$V_7 = \frac{1}{2}(x_7 - z_7)^2 \tag{54}$$

where the desired dynamics for x_7 is

$$\dot{x}_7 = -K_7(x_7 - z_7) \tag{55}$$

with a gain $K_7 > 0$. By Lyapunov function time derivative calculation, we obtain the reference z_8:

$$z_8 = C_7K_7(x_7 - z_7) - \frac{1}{R_7}(x_7 - x_9) - C_7\dot{z}_7 \tag{56}$$

Indeed the Lyapunov derivative is negative definite if the value of x_8 is properly chosen as z_8 in (56):

$$\dot{V}_7 = (x_7 - z_7)(\dot{x}_7 - \dot{z}_7) = \tag{57}$$
$$= (x_7 - z_7)\left(-\frac{1}{R_7C_7}x_7 - \frac{1}{C_7}x_8 + \frac{1}{R_7C_7}x_9 - \dot{z}_7\right)$$

$$\dot{V}_7 = -K_7(x_7 - z_7)^2 < 0 \tag{58}$$

To calculate the control input u_3 we again use backstepping technique: we can obtain it by using the Lyapunov function

$$V_8 = \frac{1}{2}(x_8 - z_8)^2 \tag{59}$$

whose time derivative is

$$\dot{V}_8 = (x_8 - z_8)(\dot{x}_8 - \dot{z}_8) = \tag{60}$$
$$= (x_8 - z_8)\left(\frac{1}{L_8}V_Su_3 - \frac{R_{08}}{L_8}x_8 - \frac{1}{L_8}x_7 - \dot{z}_8\right)$$

To have a definite positive $\dot{V}_8$ the control input must be

$$u_3 = \frac{1}{V_S}\left[x_7 + R_{08}x_8 + L_8\dot{z}_8 - L_8K_8(x_8 - z_8)\right] \tag{61}$$

with $K_8 > 0$ and constant,

$$\dot{z}_8 = C_7K_7(\dot{x}_7 - \dot{z}_7) - \frac{1}{R_7}(\dot{x}_7 - \dot{x}_9) - C_7\ddot{z}_7 \tag{62}$$

and where the function $\ddot{z}_7$ is the time derivative of $\dot{z}_7$.

$$\dot{V}_8 = (x_8 - z_8)(\dot{x}_8 - \dot{z}_8) = -K_8(x_8 - z_8)^2 < 0 \tag{63}$$

Then, using the control laws defined in (17), (39) and (61), in accordance with (37), (46), (49), (54) and (59), we have positive definite Lyapunov functions $V_{1,3} > 0$, $V_{4,6} > 0$, $V_{2,5,9} > 0$, $V_7 > 0$, $V_8 > 0$ such that their time derivatives $\dot{V}_{1,3} < 0$, $\dot{V}_{4,6} < 0$, $\dot{V}_{2,5,9} \leq 0$, $\dot{V}_7 < 0$, $\dot{V}_8 < 0$ ensure stability, according to (38), (47), (52), (58) and (63).

The composite positive definite Lyapunov function V in (16) results to have a negative semidefinite time derivative $\dot{V}$; LaSalle's theorem ensures asymptotic stability of the equilibrium x^e of entire system describing the DC microgrid:

$$\dot{V} = \dot{V}_{1,3} + \dot{V}_{4,6} + \dot{V}_7 + \dot{V}_8 + \dot{V}_{2,5,9} \leq 0 \tag{64}$$

As proven in the previous theorem, the unconstrained control laws u_1, u_2 and u_3 solve our problem. When considering a realistic application, control laws must be bounded: $u_1 \in [0,1]$, $u_2 \in [0,1]$ and $u_3 \in [0,1]$. These bounds also impose limitations for x_1^*, x_4^*, x_9^*. Bounds on x_1^* have already been considered in the theorem to have a current coming from the PV array. A bounded u_2 imposes bounds on x_9^*, $x_9^* \in (max(V_{PV}, V_B), V_S)$, and on x_4^*: $x_4^* \in [\gamma_2 V_B, \beta(x_9^*, V_B)]$, where $\gamma_2 = \frac{R_{04}}{R_4}\frac{1}{1+\frac{R_{04}}{R_4}}$ and

$$\beta(x_9^*, V_B) = \frac{x_9^* + \left(\frac{R_5}{R_4} - \frac{R_{04}}{R_4}\right)V_B}{1 + \frac{R_5}{R_4} - \frac{R_{04}}{R_4}} \tag{65}$$

When considering the bounds $u_1 \in [0,1]$ and $u_2 \in [0,1]$, bounds on the quantity R_L must be satisfied as well: indeed, given a $x_9^* > 0$, only the values of $R_L \in \Omega_{R_L}$, where

$$\Omega_{R_L} = \{R_L : x_4^* \in [\gamma_2 V_B, \beta(x_9^*, V_B)] \tag{66}$$
$$\text{for some } x_1^* \in [\gamma_1 V_{PV}, V_{PV}]\}$$

is the set such that the condition (8) is satisfied with respect to physical limitation of all the components of the circuits.

Let $X = \mathcal{R}^9$ be the state space of the closed loop system. Given the state feedback control laws $u_1 : X \to \mathcal{R}$, $u_2 : X \to$

$\mathcal{R}$, $u_3 : X \to \mathcal{R}$, in (17), (39), (61), for any value of the used gains we need to compute the maximal set

$$\Omega_K \subset X \tag{67}$$

which is invariant for the closed loop dynamical system, and is such that $u_1(z) \in [0,1]$, $u_2(z) \in [0,1]$, $u_3(z) \in [0,1]$, $\forall z \in \Omega_K$. Such a maximal set is well defined, because the family of all invariant set in X is closed under union. The set Ω_K is hard to describe, but we can ensure that it is not empty.

Theorem 2: For any $R_L \in \Omega_{R_L}$, $\forall\ x_1^* \in [\gamma_1 V_{PV}, V_{PV}]$: $x_4^* \in [\gamma_2 V_B, \beta(x_9^*, V_B)]$, $\forall\ x_9^*$ such that $max(V_{PV}, V_B) < x_9^* < V_S$ there exist gains K_1, $\overline{K}_1$, K_1^α, K_3, $\overline{K}_3$, K_3^α, K_4, $\overline{K}_4$, K_4^α, K_6, $\overline{K}_6$, K_6^α, K_7, K_8 such that $\Omega_K \neq \emptyset$.

Proof 2: To prove controller existence, let us now consider the controllers u_1 and u_2 where no integral error correction terms are considered: the value of the gains $\overline{K}_1$, K_1^α, $\overline{K}_3$, K_3^α, $\overline{K}_4$, K_4^α, $\overline{K}_6$, K_6^α, is set to be zero. As we are neglecting the integral error dynamics, stability conditions to be respected are stated only by the formulas in (31) and (32). A choice of K_1 and K_3 (K_4 and K_6) respecting these conditions is done: $K_1 = \frac{1}{R_1 C_1}$ and $K_3 = \frac{R_{01}}{L_3}$ ($K_4 = \frac{1}{R_4 C_4}$ and $K_6 = \frac{R_{04}}{L_6}$). A simple choice of K_7 and K_8 respecting stability is $K_7 = \frac{1}{R_7 C_7}$ and $K_8 = \frac{R_{08}}{L_8}$. The conditions $x_1^* \in [\gamma_1 V_{PV}, V_{PV}]$, $x_4^* \in [\gamma_2 V_B, \beta(x_9^*, V_B)]$, $R_L \in \Omega_{R_L}$, $max(V_{PV}, V_B) < x_9^* < V_S$ implies that x^e is an equilibrium with $u_1(x^e) \in [0,1]$, $u_2(x^e) \in [0,1]$, $u_3(x^e) \in [0,1]$. Therefore $x^e \in \Omega_K$.

Corollary 3: For any given $R_L \in \Omega_{R_L}$, $\forall\ x_1^* \in [\gamma_1 V_{PV}, V_{PV}]$: $x_4^* \in [\gamma_2 V_B, \beta(x_9^*, V_B)]$, $\forall\ x_9^*$ such that $max(V_{PV}, V_B) < x_9^* < V_S$, given the state feedback control laws u_1, u_2, u_3, defined in (17), (39), (61), and for any initial state in Ω_K, the state $z(t)$ of the closed loop system asymptotically converges to x^e, and $u_1(z(t)) \in [0,1]$, $u_2(z(t)) \in [0,1]$, $u_3(z(t)) \in [0,1]$, $\forall t \geq 0$.

V. SIMULATION RESULTS

In this section we present some simulations that show the results obtained using the proposed control inputs. Such simulations are obtained using Matlab. The values of the parameters for the model are depicted in Tables II. The simulation target is to correctly feed a load and to maintain the grid stability, which means to ensure no large variation in the DC grid voltage. The simulation time is twenty seconds. The considered reference value x_9^* for the DC grid voltage is selected as $x_9^* = 1000\ V$. A secondary controller is supposed to provide the references to be reached each time interval; during that period the introduced control laws will bring the devices to operate in the desired points. The selected strategy assign to the PV and battery the duty to fulfill the losses into the network; the references will then be calculated according to the load current. The references are updated every second: during the first ten seconds the load is supposed to not vary during each time interval of a second.

We can split the simulation in two parts: in the first one, which is from zero to ten seconds, the voltages of the PV array and of the battery are constant and the load resistance piecewise constant. Furthermore, the references provided by

Table II
GRID PARAMETERS.

Parameter	Value	Parameter	Value
C_1	0.1 F	L_3	0.033 H
C_2	0.01 F	R_{01}	0.01 Ω
R_1	0.1 Ω	R_{02}	0.01 Ω
R_2	0.1 Ω	C_4	0.1 F
C_5	0.01 F	R_{04}	0.01 Ω
R_4	0.1 Ω	R_{05}	0.01 Ω
R_5	0.01 Ω	L_6	0.033 H
C_7	0.01 F	L_8	0.0033 H
R_{07}	0.01 Ω	R_{08}	0.01 Ω
R_7	0.1 Ω	C_9	0.0001 F

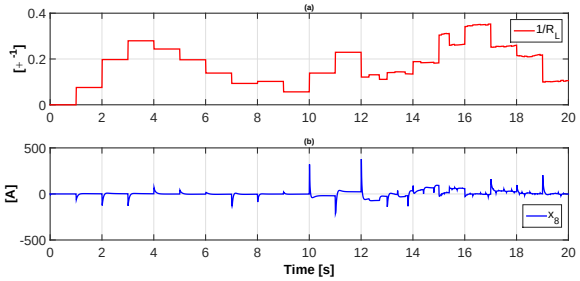

Figure 3. The load resistance $\frac{1}{R_L}$ in (a) and the current x_8 in (b).

the higher level controller are exact and the supercapacitor is needed only for providing grid stability during the transient time needed by the converters that are connected to the PV and the battery. In the second part of the simulation, in addition to the step variation, the load is supposed to be time varying and disturbances acting on the PV voltage are considered (see Figure 4). To better represent any possible case, we have also simulated the case where the references do not fulfill the energy balance: there the supercapacitor will need to provide power during all the time window. Figure 3 describes the values of the resistance $\frac{1}{R_L}$ over the time; we can see the described behaviour, which is piecewise constant for ten seconds and then becomes time-varying. In accordance to the values of $\frac{1}{R_L}$, the references x_1^* and x_4^* are obtained for the power balance target. As depicted in Figure 5, the C_1 and C_4 capacitor voltages reach the desired values during the considered time step. Here two different situations for the controllers are faced because the two devices need two different treatments; we need from the PV array to start providing the highest level of power as soon as possible,

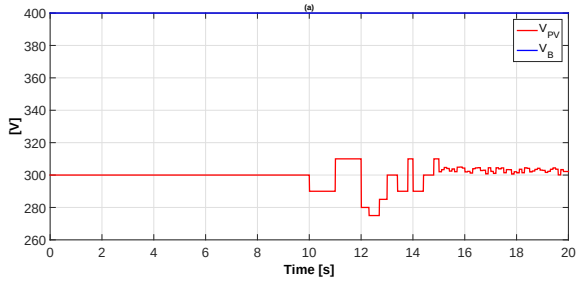

Figure 4. The voltages of V_{PV} (red line) and V_B (blue line).

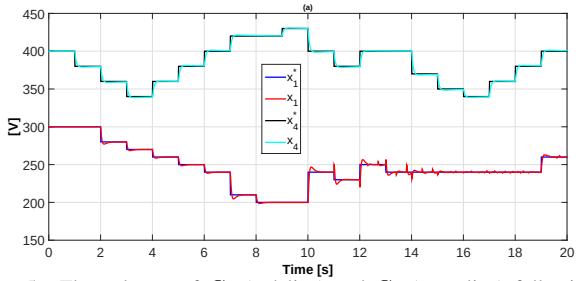

Figure 5. The voltages of C_1 (red line) and C_4 (cyan line) following the desired references, the blue and black lines, respectively.

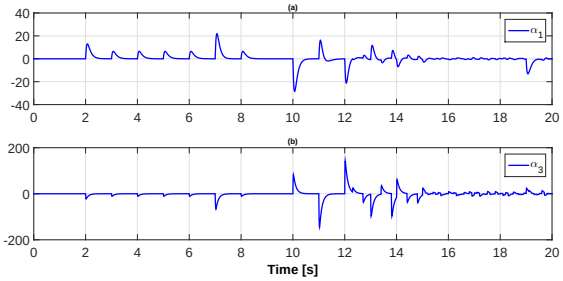

Figure 6. The integral terms used by the control law u_1: in (a) α_1, in (b) α_3.

while the battery needs to have a smooth behaviour to preserve its life-time. The integral terms in the control action are introduced in Figures 6 and 7; the considered eigenvalues for the systems are different because of the different targets. We note that both the charge and discharge battery situations are faced. Here we considered the voltage of the battery not to be affected by the current behaviour; indeed a constant value is used to represent it because the battery is supposed to be sized in such a way that it is not affected by current dynamics over a time of twenty seconds. The resulting voltage dynamics on the grid connected capacitors, C_2 and C_5, are modified by the current flow generated by the sources; all the dynamics are stable, as shown in Figure 8. Their evolution is influenced by the value of the DC grid voltage, which is the capacitor C_9: its value over time is depicted in Figure 9. To satisfy stability constraints, in response to the load variations and to the missing power coming from the PV and the battery, the voltage of the capacitor C_7 reacts balancing the energy variation. Figure 10 describes the currents generated from

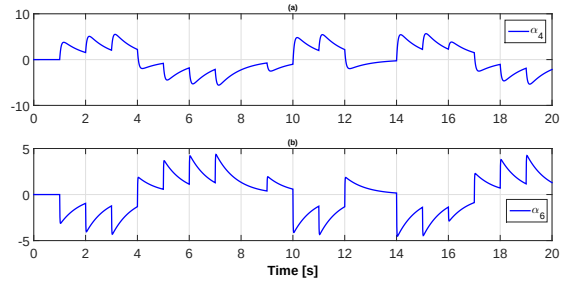

Figure 7. The integral terms used by the control law u_2: in (a) α_4, in (b) α_6.

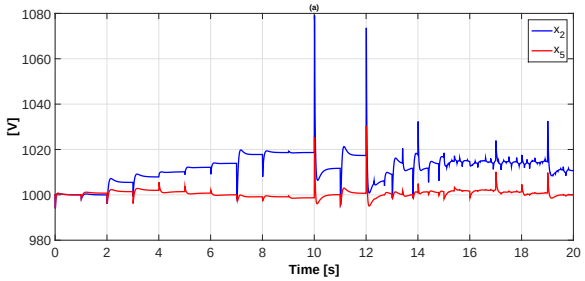

Figure 8. The voltages of C_2 (blue line) and C_5 (red line).

the PV and the battery: these dynamics are dependent on the voltages and related to them.

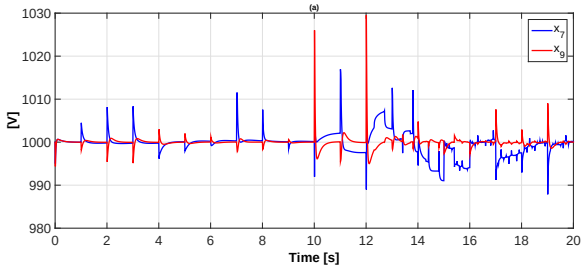

Figure 9. The voltages of C_7 (blue line) and C_9 (red line).

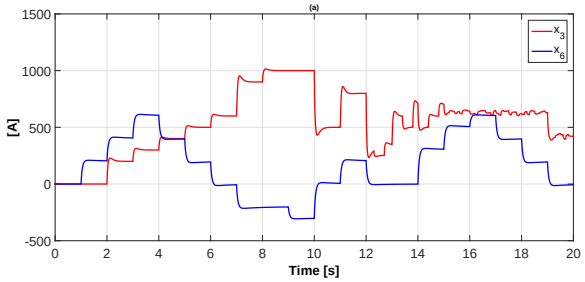

Figure 10. The currents x_3 (red line) and x_6 (blue line).

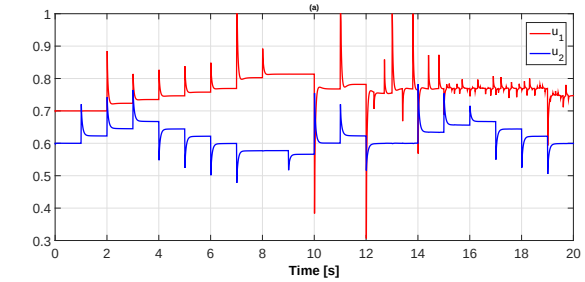

Figure 11. The control inputs u_1 (red line) and u_2 (blue line).

Figure 11 introduces the generated control inputs u_1 and u_2, that are bounded by the devices to be between zero and one, while Figure 4 shows the voltages of the PV array and of the battery. The control inputs are smooth except in the case of reference step variations. The control input for the DC/DC converter connected to the supercapacitor is depicted

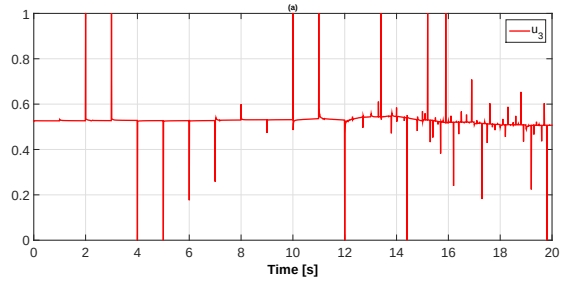

Figure 12. The control input u_3.

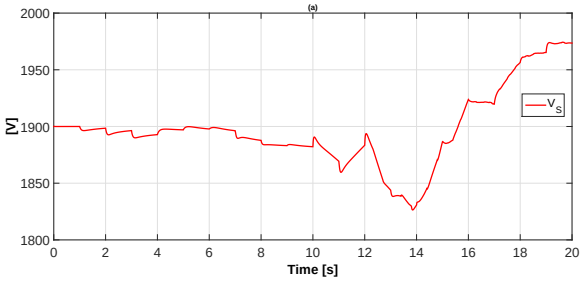

Figure 13. The voltage of the supercapacitor.

in Figure 12: its variation depends on the variations of voltage V_S (see Figure 13) and of the load (see Figure 3). As results, the desired voltage for the DC microgrid is always kept (Figure 9). The developed control strategy is then shown to successfully operate in a wide range of situations: constant and time-varying load, acting of perturbation on the sources and big step variations of the references.

VI. CONCLUSIONS

In this paper a realistic DC MicroGrid composed by a PV array, two storage devices, a load and their connected devices is modeled. It is controlled in order to correctly provide a desired amount of power for feeding an uncontrolled bounded load while ensuring a desired grid voltage value. Hypotheses on the ad hoc size of the components are done to physically allow the power exchange. Stability analysis is carried out for the complete system and physical limitations are also considered. Simulations show the robustness of the adopted control action both during the transient and in steady-state operation mode in case of constant or time-varying load.

REFERENCES

[1] M. A. Eltawil and Z. Zhao, "Grid-connected photovoltaic power systems: Technical and potential problemsa review," *Renewable and Sustainable Energy Reviews*, vol. 14, no. 1, pp. 112 – 129, 2010.

[2] J. Barton and D. Infield, "Energy storage and its use with intermittent renewable energy," *Energy Conversion, IEEE Transactions on*, vol. 19, pp. 441–448, June 2004.

[3] G. Krajai, N. Dui, Z. Zmijarevi, B. V. Mathiesen, A. A. Vuini, and M. da Graa Carvalho, "Planning for a 100% independent energy system based on smart energy storage for integration of renewables and co_2 emissions reduction," *Applied Thermal Engineering*, vol. 31, no. 13, pp. 2073 – 2083, 2011.

[4] R. Lasseter and P. Paigi, "Microgrid: a conceptual solution," in *Power Electronics Specialists Conference, 2004. PESC 04. 2004 IEEE 35th Annual*, vol. 6, pp. 4285–4290 Vol.6, June 2004.

[5] P. Piagi and R. Lasseter, "Autonomous control of microgrids," in *Power Engineering Society General Meeting, 2006. IEEE*, pp. 8 pp.–, 2006.

[6] N. Hatziargyriou, H. Asano, R. Iravani, and C. Marnay, "Microgrids," *Power and Energy Magazine, IEEE*, vol. 5, pp. 78–94, July 2007.

[7] T. Dragicevic, J. Vasquez, J. Guerrero, and D. Skrlec, "Advanced lvdc electrical power architectures and microgrids: A step toward a new generation of power distribution networks.," *Electrification Magazine, IEEE*, vol. 2, pp. 54–65, March 2014.

[8] J. Guerrero, P. C. Loh, T.-L. Lee, and M. Chandorkar, "Advanced control architectures for intelligent microgrids part ii: Power quality, energy storage, and ac/dc microgrids," *Industrial Electronics, IEEE Transactions on*, vol. 60, pp. 1263–1270, April 2013.

[9] H. J. Sira Ramirez and R. Silva-Ortigoza, *Control design techniques in power electronics devices*. Springer, 2006.

[10] S. Mariethoz, S. Almer, M. Baja, A. Beccuti, D. Patino, A. Wernrud, J. Buisson, H. Cormerais, T. Geyer, H. Fujioka, U. Jonsson, C.-Y. Kao, M. Morari, G. Papafotiou, A. Rantzer, and P. Riedinger, "Comparison of hybrid control techniques for buck and boost dc-dc converters," *Control Systems Technology, IEEE Transactions on*, vol. 18, pp. 1126–1145, Sept 2010.

[11] Y. Chen, G. Damm, A. Benchaib, and F. Lamnabhi-Lagarrigue, "Multi-time-scale stability analysis and design conditions of a vsc terminal with dc voltage droop control for hvdc networks," in *53rd IEEE Conference on Decision and Control*.

[12] Y. Chen, G. Damm, A. Benchaib, M. Netto, and F. Lamnabhi-Lagarrigue, "Control induced explicit time-scale separation to attain DC voltage stability for a VSC-HVDC terminal," in *19th IFAC World Congress on International Federation of Automatic Control (IFAC 2014)*, vol. 19, (Cape Town, South Africa), pp. 540–545, Aug. 2014.

[13] A. P. N. Tahim, D. J. Pagano, E. Lenz, and V. Stramosk, "Modeling and stability analysis of islanded dc microgrids under droop control," *IEEE Transactions on Power Electronics*, vol. 30, no. 8, pp. 4597–4607, 2015.

[14] A. Bidram, A. Davoudi, F. L. Lewis, and J. M. Guerrero, "Distributed cooperative secondary control of microgrids using feedback linearization," *IEEE Transactions on Power Systems*, vol. 28, no. 3, pp. 3462–3470, 2013.

[15] G. Walker and P. Sernia, "Cascaded dc-dc converter connection of photovoltaic modules," *Power Electronics, IEEE Transactions on*, vol. 19, pp. 1130–1139, July 2004.

[16] D. Marx, P. Magne, B. Nahid-Mobarakeh, S. Pierfederici,

and B. Davat, "Large signal stability analysis tools in dc power systems with constant power loads and variable power loads; a review," *Power Electronics, IEEE Transactions on*, vol. 27, pp. 1773–1787, April 2012.

[17] D. Hamache, A. Fayaz, E. Godoy, and C. Karimi, "Stabilization of a dc electrical network via backstepping approach," in *Industrial Electronics (ISIE), 2014 IEEE 23rd International Symposium on*, pp. 242–247, June 2014.

[18] D. Olivares, A. Mehrizi-Sani, A. Etemadi, C. Canizares, R. Iravani, M. Kazerani, A. Hajimiragha, O. Gomis-Bellmunt, M. Saeedifard, R. Palma-Behnke, G. Jimenez-Estevez, and N. Hatziargyriou, "Trends in microgrid control," *Smart Grid, IEEE Transactions on*, vol. 5, pp. 1905–1919, July 2014.

[19] S. Sanders, J. Noworolski, X. Liu, and G. C. Verghese, "Generalized averaging method for power conversion circuits," *Power Electronics, IEEE Transactions on*, vol. 6, pp. 251–259, Apr 1991.

[20] R. Middlebrook and S. Cuk, "A general unified approach to modelling switching-converter power stages," *International Journal of Electronics*, vol. 42, no. 6, pp. 521–550, 1977.

[21] D. Lifshitz and G. Weiss, "Optimal control of a capacitor-type energy storage system," *Automatic Control, IEEE Transactions on*, vol. 60, pp. 216–220, Jan 2015.

[22] P. Kundur, J. Paserba, V. Ajjarapu, G. Andersson, A. Bose, C. Canizares, N. Hatziargyriou, D. Hill, A. Stankovic, C. Taylor, T. Van Cutsem, and V. Vittal, "Definition and classification of power system stability ieee/cigre joint task force on stability terms and definitions," *Power Systems, IEEE Transactions on*, vol. 19, pp. 1387–1401, Aug 2004.

[23] P. Kundur, N. J. Balu, and M. G. Lauby, *Power system stability and control*. McGraw-Hill, 1994.